Low temperature properties of hard elastic polypropylene fibres

Yizhan Zhu, Norimasa Okui*, Toshiaki Tanaka, Susumu Umemoto and Tetuya Sakai†

Department of Organic and Polymeric Materials, Tokyo Institute of Technology, Ookayama, Meguroku, Tokyo 152, Japan

(Received 30 July 1990; revised 18 September 1990; accepted 2 October 1990)

The temperature dependence of hard elastic polypropylene fibre was studied in the temperature range −140°C to 20°C. The third yield point was found on the stress–strain curve below the glass transition temperature, as were the first and second yield points. The yield behaviours for the first and third points depended strongly on the temperature and changed remarkably at the glass transition temperature. The first, second and third yield behaviours were associated with, respectively, the initial deformation of the total stacked lamellar structure, the onset of unfolding of the lamellar crystal, and the deformation of the amorphous chains between lamellae after the lamellar separation.

(Keywords: polypropylene; glass transition; yielding; hard elastic)

INTRODUCTION

It is well known that the well-developed stacked lamellar structure along the fibre axis can be obtained by stress-induced crystallization[1–4]. Such lamellar structure exhibits a high elastic recovery with an energetic elasticity and is termed a hard elastic or springy material. In particular, the hard elastic material shows high elastic recovery even at temperatures well below the glass transition temperature (T_g)[5]. Many papers and reviews[4–12] of hard elastic fibres have focused on the relationships between the stacked lamellar structure and the mechanical properties. However, little attention has been paid to the hard elastic properties in the low temperature ranges, especially in the vicinity of T_g. In this paper, the hard elastic properties of polypropylene fibres are studied with special reference to the low temperature range from −140°C to 20°C.

EXPERIMENTAL

Isotactic polypropylene fibres were prepared by high speed melt spinning[12,13] with a take-up speed of 1000 m min^{-1} at an extrusion temperature of 230°C. The as-spun fibres were annealed at 140°C in the free state for 1 h. The density and birefringence of the annealed fibres were 0.908 g cm^{-3} and 0.021, respectively.

Mechanical testing was carried out by straining the fibres at a strain rate of 0.6 min^{-1} in a tensile tester equipped with a temperature box which could be kept at temperatures ranging from −150°C to 80°C with an accuracy of ±1°C. Stress–strain curves were recorded for loading and unloading with the same strain rate in the temperature range from −140°C to 20°C. The dynamic mechanical properties were measured at a constant frequency of 3 Hz and at a heating rate of 2°C min^{-1} in the range −130°C to 20°C with a rheolograph (Toyoseiki Co.).

RESULTS AND DISCUSSION

Temperature dependence of stress–strain curve

Figure 1 shows the temperature dependence of the dynamic modulus from −130°C to 20°C. The storage modulus decreases gradually but drops markedly with rise in temperature above −40°C. The loss modulus shows a clear single peak starting at about −40°C with a maximum at about −10°C and tailing off at about 10°C. The glass transition temperature of isotactic polypropylene is generally found in a similar temperature range[14].

Figure 2 shows the stress–strain curves measured at various temperatures from −100°C to 20°C. At 20°C, the fibres show a typical stress–strain curve with the hard elastic characteristics showing the first and second yield points on the loading curve and a sharp decrease in stress followed by a plateau-like stress region on the unloading curve. The stress increases with decrease in temperature, clearly exhibiting a first yield point and subsequently a new yield point (the third yield point) which is found just after the first yielding. This can be clearly seen on the loading curve at −100°C. The first and third yield points appear, respectively, at ~5% and ~15% of strain at temperatures below T_g; however, their strains strongly depend on temperature. The second yield point appears at ~75% strain but is not as clear as the first and third points. On the other hand, the abrupt stress reduction after the plateau-like stress region on the unloading curve becomes obscure and the residual strain increases with a decrease of temperature, especially below T_g.

Figure 3 shows a schematic illustration of the stress–strain curve obtained at temperatures well below T_g. In the loading curve (OABCDE), A, B and D represent the first, third and second yield points, respectively. The loading curve can be divided into four

* To whom correspondence should be addressed
† Present address: Department of Home Science, Kyoritu Women's University, Chiyodaku, Tokyo, Japan

0032-3861/91/142588-06

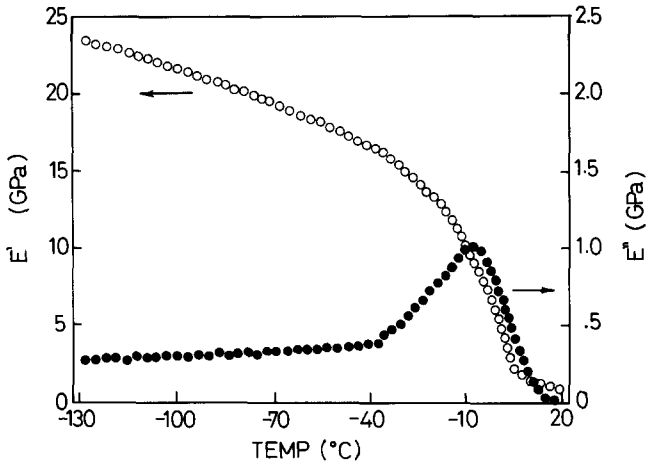

Figure 1 Temperature dependence of dynamic moduli. ○, Storage modulus; ●, loss modulus

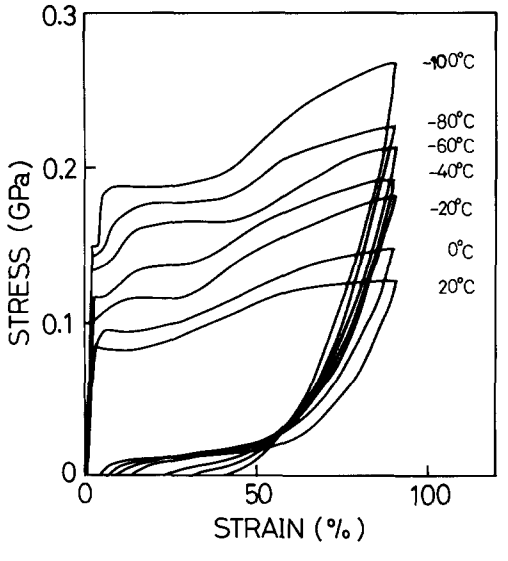

Figure 2 Stress–strain curves at various temperatures

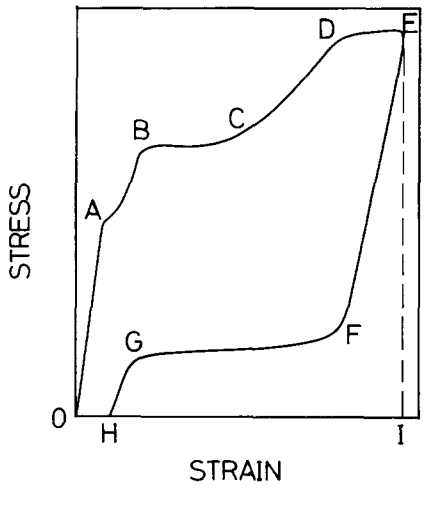

Figure 3 Typical stress–strain curve for hard elastic fibre. A, B and D denote the first, third and second yield points, respectively

stages. In stage 1 (OA), the fibre exhibits a nominal Hookian behaviour (so-called initial Young's modulus) followed by the clear yield point A which can be strongly related to the whole stacked lamellar structure constructed with the lamellar crystals and the amorphous layer. In stage 2 (AB), many investigations have shown that the separation of the stacked lamellae leads to microvoid formation after the first yielding[4–12]. The appearance of the third yield point at temperatures below T_g suggests that the lamellar separation occurs first and then the glassy amorphous chains between the separated lamellae are deformed. In other words, there are two factors involved in the lamellar separation process: adhesive fracture mechanics[15], and the deformation of amorphous molecules between lamellae. The deformation of the amorphous layer may be associated with the deformation of tie chains, folded chain loops, cilia and floating chains (which are unattached to any crystalline region) between lamellae and others[16]. The adhesive fracture commences at a critical yield stress and leads to void opening. The amorphous contribution to the yield behaviour is strongly dependent on temperature, especially at the glass transition region from the glassy state to the rubbery state. At temperatures below T_g, the amorphous contribution to the stress may be larger than the adhesive fracture energy and thus the stacked lamellae may separate before the yielding of the glassy amorphous molecules, which is similar to the yield behaviour generally observed in a glassy polymer[17]. Consequently it could be thought that the stress–strain curve shows the first and the third yield behaviours.

In stage 3 (BCD), the lamellar separation with large horizontal void formation predominates and the interlamellar tie chains are oriented to the extension direction. The second yield point D is the signal of the onset of plastic deformation of the crystal lamellae, that is the onset of unfolding of lamellae[7,11,12]. In stage 4 (DE), plastic deformation predominates with pulling of fibrils from lamellar crystals. The residual strain increases drastically from this stage and the elastic recovery becomes very poor[11,12].

The unloading curve (EFGH) can also be divided into three regions which are characterized by the steep stress reduction region (EF), the plateau-like stress region (FG) and the cascade-like stress reduction at the end of the unloading curve (GH). OH is the residual strain, and the elastic recovery is defined as the ratio of (HI/OI). It is clear that the temperature dependence of the stress–strain curve is strongly related to T_g.

Temperature dependence of modulus and yield stress

The moduli E_1, E_2 and E_3 were calculated from the slope of OA, CD and AB, respectively, and the yield stresses σ_1, σ_2 and σ_3 were obtained from the points A, D and B, respectively, on the stress–strain curve (*Figure 3*). (E_2 may not be strictly defined as the modulus, but is dealt with as a nominal modulus in this paper.) The values of modulus and yield stress thus obtained are plotted against temperature in *Figures 4* and *5*, respectively. With decreasing temperature, the moduli E_1 and E_3 change significantly at the glass transition regions from 0°C to −40°C, while the modulus E_2 shows almost linear temperature dependence. E_1 is much larger than E_2 and E_3. The value of E_1 varies from ~5 to ~17 GPa, E_2 from ~0.1 to ~0.3 GPa and E_3 from ~0.1 to ~0.6 GPa with decreasing temperature from 20°C to −100°C.

The yield stresses σ_1, σ_2 and σ_3 show almost linear temperature dependence. It is interesting to note that the σ_2–temperature relationship extrapolates to zero near

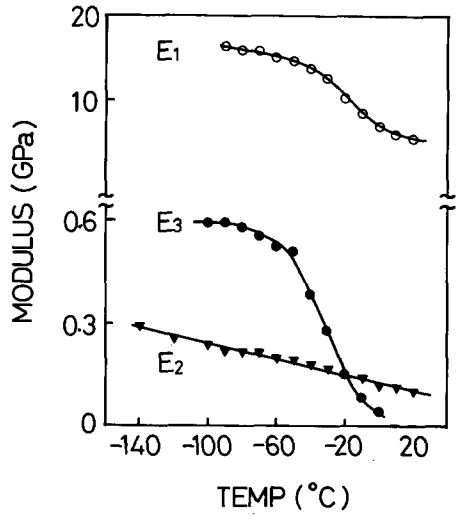

Figure 4 Temperature dependence of moduli of E_1, E_2 and E_3, obtained from the slope of OA, CD and AB, respectively, in *Figure 3*

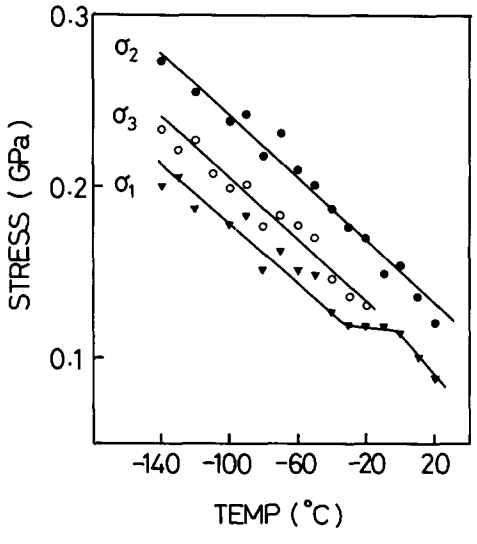

Figure 5 Temperature dependence of yield stresses σ_1, σ_2 and σ_3 obtained from the points A, D and B, respectively, in *Figure 3*

the melting temperature. σ_2 is the yield stress in the direction parallel to the fibre axis of hard elastic fibre and is associated with the necking stress of the stacked lamellar structure. The value of σ_2 is about 10 times larger than that of the generally observed yield stress for the non-oriented crystalline polypropylene[18]. This might be caused by the angular dependence of the yield stress. The yield stress in the directions parallel and perpendicular to the fibre axis of oriented polypropylene are reported to be ~255 MPa and 29 MPa, respectively[19]. That is, the yield stress parallel to the fibre axis is about 10 times larger than that perpendicular to the fibre axis. It is also interesting to note that the temperature dependence of σ_1 shows a break point in the glass transition region and fits the extrapolated line of σ_3 above T_g. This suggests that in the temperature regions above T_g the adhesive fracture energy is much larger than the amorphous contribution to the yield stress, because the amorphous chains are in the rubbery state. The amorphous contribution to the yield stress increases with decreasing temperature, especially below T_g. In other words, the lamellar separation and the yielding of the amorphous chains between lamellae occur independently.

It is assumed that a simple mechanical model is applicable to the modulus, as proposed in *Figure 6*, where E_c is the axial crystal modulus and E_a is the axial amorphous modulus. E_v is the axial modulus for the adhesive fracture and can be neglected after the first yielding. The axial elastic modulus E is given by:

$$1/E = X_c/E_c + (1 - X_c)/(\alpha_a E_a + (1 - \alpha_a)E_v) \quad (1)$$

where X_c is the volume crystallinity of the sample and α_a is the fraction of amorphous phase between lamellae, which is constructed from the amorphous chains, such as tie chains, cilia, folded chain loops and floating chains. The first modulus E_1 can be expressed by equation (1) and the third modulus E_3 can be simplified to:

$$1/E_3 = X_c/E_c + (1 - X_c)/\alpha_a E_a \quad (2)$$

The amorphous chain contribution to E_a can be divided roughly into two factors: the first is in the case of chains which are not attached to different lamellae (cilia, loops and floating chains) and the second is the tie chain contribution (E_t). At temperatures below T_g, the amorphous chains are all in the glassy state and show yield behaviour (the third yielding). The region after the third yielding is attributed to strain or work softening and further extensions give rise to orientation and flow of amorphous chains. The orientation of amorphous chains, especially tie chains, can contribute to the slope of the stress–strain curve (E_2). Therefore E_2 can be approximated to:

$$1/E_2 = X_c/E_c + (1 - X_c)/\beta E_t \quad (3)$$

where β is the fraction of tie chains in the amorphous phase.

Values of E_a, E_t and E_v can be estimated from the data of moduli E_1, E_2 and E_3 and the crystallinity ($X_c = 0.68$). Here, the degree of crystallinity and the crystal modulus of 42 GPa (ref. 20) are assumed to be independent of temperature. At temperatures well below T_g, such as -100°C, it is also assumed that E_a and E_t have the same value, of about 2 GPa, which is found for the glassy state of atactic polypropylene[21]. The values of α_a and β were estimated to be ~0.1 and ~0.04 respectively, on the basis of the modulus data at -100°C.

The values of the moduli thus estimated are plotted as a function of temperature in *Figure 7*. The moduli of

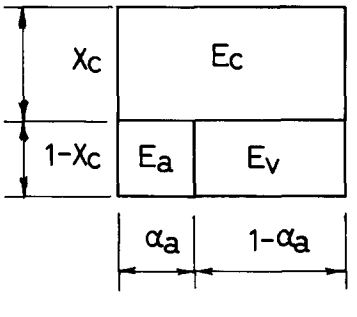

Figure 6 Mechanical model for stacked lamellar structure. E_c is the axial crystal modulus of lamellar crystal, E_a is the modulus of amorphous phase between lamellae, E_v is the modulus of the adhesive fracture, which is associated with lamellar separation. X_c and α_a are the volume crystallinity and the fraction of amorphous phase between lamellae, respectively

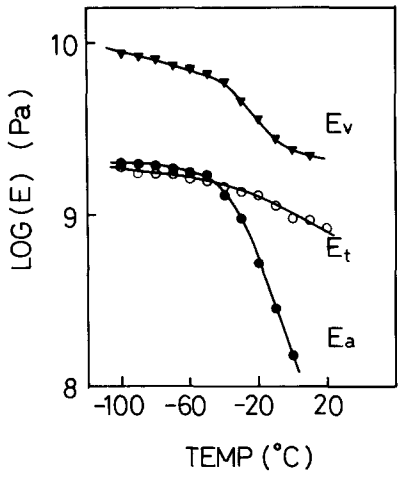

Figure 7 Temperature dependence of estimated moduli E_v, E_a and E_t, associated with adhesive fracture, amorphous contribution and tie chain contribution, respectively

E_a and E_v change clearly in the T_g region. The value of E_a and its temperature dependence are consistent with those for the amorphous atactic polypropylene[21]. It is interesting to note that the temperature dependence of E_t is much less than that of E_a. The amorphous contribution to the temperature dependence of the modulus can be controlled by the type of amorphous chains, i.e. whether the chains are bridged from one lamella to another or are not attached to different lamellae. The latter type of amorphous chains show a similar temperature dependence to non-crosslinked amorphous polymers. The tie chain contribution to the modulus is similar to crosslinked rubbery materials. The distribution of the tie chain length can be related to the number-average molecular weight of the network chain between crosslinks. Therefore, the temperature dependence of the modulus is smaller the shorter the length of the tie chain.

The magnitude of E_v may be a measure of the contribution to the complex interlamellar structure. The interlamellar structure is composed not only of the amorphous chains discussed above but also of the a^*-axis oriented crystals. The elastic crystal modulus parallel to the a^*-axis lies at ~ 3 GPa (ref. 20). The other contributions to E_v include the effect of van der Waal's forces, the free energy of the chain folded surface, the lamellar beam bending event, the flaw density distribution, the initiation of propagating adhesive failure sites and others[15]. Detailed studies on E_v to obtain experimental data are required for further discussion.

Temperature dependence of strain at yield point

Figure 8 shows three yield strains, ε_1, ε_2 and ε_3 corresponding to the strains due to the yield points A, D and B, respectively. The temperature dependence of the yield strain shows a break point at the glass transition temperature for ε_1 and ε_3 but not for ε_2. Below T_g, the temperature dependence of ε_1 and ε_3 are very small, and the values of their slopes are $\sim 7.5 \times 10^{-6}\,K^{-1}$ for ε_1 and $\sim 2 \times 10^{-5}\,K^{-1}$ for ε_3. Their slopes above T_g are larger: $\sim 5.2 \times 10^{-4}\,K^{-1}$ for ε_1 and $\sim 1.6 \times 10^{-2}\,K^{-1}$ for ε_3. On the other hand, the second yield strain shows linear temperature dependence, although the data are scattered. The value of the slope for ε_2 is $\sim 3 \times 10^{-4}\,K^{-1}$. The slopes could be associated with the thermal expansion coefficient of the fibre. In fact, the values of the slopes for ε_1 and ε_3 below T_g lie in the same order as the thermal expansion coefficient, α, of polypropylene below T_g ($\alpha = 6.5 \times 10^{-5}\,K^{-1}$)[14]. In addition, the values for ε_1 above T_g and for ε_2 are in the same order as α above T_g ($\alpha = 1.05$–$1.4 \times 10^{-4}\,K^{-1}$)[14]. The value for ε_3 above T_g, however, is 100 times larger than α. This high value may be caused by the large expansion of the voids between lamellae. These positive values are due to the intermolecular expansion of amorphous chains between lamellae. On the contrary, the expansion coefficient along the chain axis in the lamellar crystal shows a negative value of -6.42×10^{-5} (ref. 22).

The yield strain of ε_2 is closely associated with the onset of pulling out of fibrils from lamellae. In other words, ductility of amorphous tie chains between lamellae plays an important role in determining the critical second strain. Here, one could assume that the second yield strain is expressed as a function of the draw ratio of the tie chains between lamellae (λ_a):

$$\varepsilon_2 = \lambda_a l_a / l_0 \tag{4}$$

where l_a and l_0 are the thickness of amorphous layer and the long spacing in the original stacked lamellar structure respectively. The ratio of l_a/l_0 can be simply assumed to be $(1 - X_c)$, where X_c is the degree of crystallinity. Therefore, one could obtain the draw ratio of the tie chain (λ_a) from the experimental data of ε_2 and X_c. For example, ε_2 and X_c are 0.75 and 0.68 respectively, in this work so that the value of λ_a is ~ 2.3. If the value of λ_a can be applied to the stacked lamella of polyethylene fibre with $\sim 90\%$ crystallinity, ε_2 is ~ 0.23 which is much smaller than the value for the hard elastic polypropylene fibre. The amorphous contribution to the hard elastic properties is thus an important factor.

Temperature dependence of residual strain and elastic recovery

The residual strain (OH) and the slope of the last stage on the unloading curve (GH), as shown in *Figure 3*, will be referred to as ε_4 and E_4, respectively. *Figure 9* shows the temperature dependence of the residual strain (ε_4)

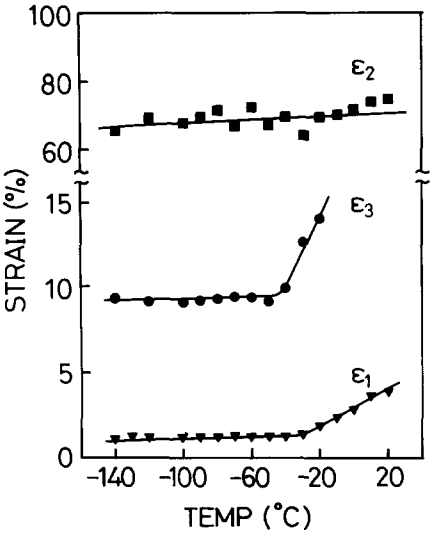

Figure 8 Temperature dependence of yield strains ε_1, ε_2 and ε_3, corresponding to strains due to yield points A, D and B, respectively, in *Figure 3*

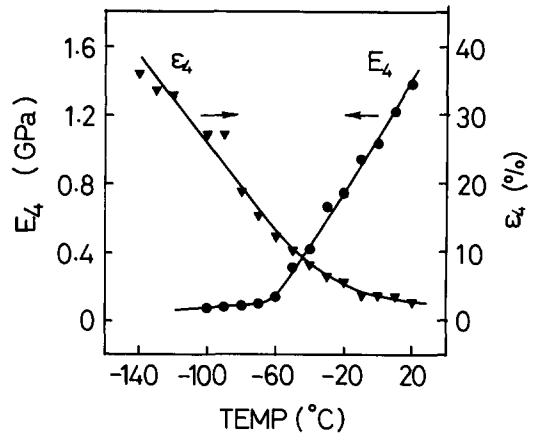

Figure 9 Temperature dependence of modulus E_4 and residual strain of ε_4, obtained from the slope GH and residual strain OH, respectively, in *Figure 3*

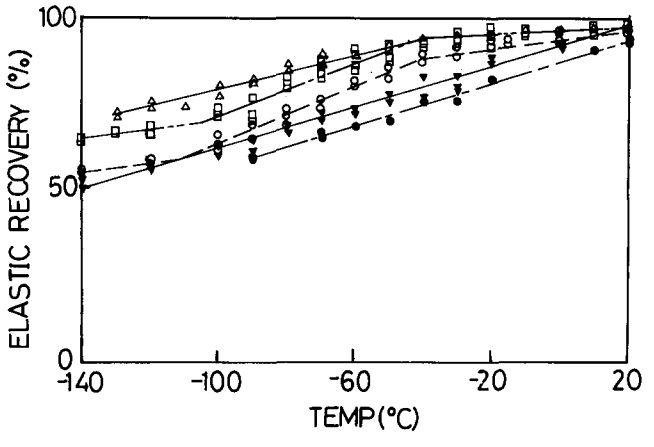

Figure 10 Temperature dependence of amorphous layer between lamellae on elastic recovery from various extensions: Δ, 30%; □, 50%; ○, 70%; ▼, 90%; ●, 100%

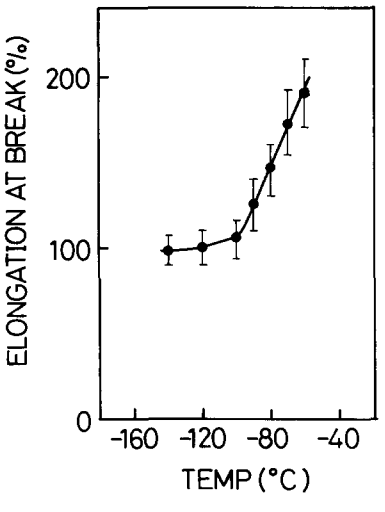

Figure 11 Temperature dependence of elongation at break

and the slope (E_4) after 50% extension. The values of ε_4 and E_4 vary remarkably in the vicinity of T_g. The large residual strain below T_g indicates the frozen amorphous chains and the large temperature dependence suggests the large distribution of molecular conformational energy in the amorphous layer between lamellae. The shape of the stress–strain curve below T_g is similar to that for crazed polystyrene[23]. This means that the amorphous chain contribution to the hard elastic polypropylene is similar to the crazed fibril contribution to the hard elastic polystyrene, because both are in the glassy state.

The plateau-like recovery region (FG) disappears below T_g. This region may be considered as a result of the thermal expansion stress due to the thermal motions of the amorphous molecules between lamellae. Such thermal motions cease below T_g and the plateau-like region then disappears. On the other hand, the cascade-like stress reduction (GH) at the end of the unloading curve above T_g is due to the formation of the rigid phase in the interlamellar region. During the unloading process above T_g, the highly strained amorphous chains between lamellae will be relaxed and subsequently crystallized to the a^*-axis oriented crystals, or the inclined a^*-axis oriented crystals will rotate perpendicular to the lamellar surface[7]. Such a^*-axis oriented crystals might be associated with the rigid phase between lamellae and can contribute to the cascade-like stress reduction at the end of the unloading curve.

The temperature dependence of the amorphous layer between lamellae on elastic recovery is shown in *Figure 10*. The temperature dependence of the elastic recovery shows two break points at about −40°C and about −100°C. The increase in the slope in *Figure 10* below T_g is due to the same mechanism as for ε_4 in *Figure 9*. However, the elastic recovery depends not only on the temperature but also on the degree of extension of the fibre. Below the critical extension (ε_2) of 75%, discussed above, the elastic recovery is more than 95% and its temperature dependence is small. On the contrary, above the critical extension, the elastic recovery decreases and its temperature dependence becomes greater. These results also arise from the deformation behaviour in the amorphous layer and the destruction of the lamellar structure.

Changes in the temperature dependence of the elastic recovery at extension above 50%, found at about −100°C in *Figure 10*, could be related to the ductility of the fibres. That is, the elongation at break depends on temperature, as shown in *Figure 11*, in which a break point at about −100°C is found. It is generally observed that the elongation at break is affected strongly by the γ-relaxation, which is associated with the local mode in polypropylene molecules. The γ-relaxation temperature is reported to be about −80°C (ref. 14). Therefore, the break points at about −100°C in *Figures 10* and *11* are closely associated with the γ-relaxation mechanism.

CONCLUSION

The temperature dependence of hard elastic polypropylene fibre was studied in the temperature range −140°C to 20°C. At temperatures above T_g, there were two yield points on the stress–strain curve, i.e. the first and second yieldings. However, below T_g the third yield point was found just after the first yielding in addition to the first and the second yield points. The behaviours of the first and third yielding depend strongly on the temperature and changed remarkably at the glass transition temperature. The first yielding is related to the whole stacked lamellar structure constructed with the lamellar crystals and the amorphous layer. After the first yielding, the separation of the stacked lamellae leads to microvoid formation. The second yielding signals the

onset of unfolding of lamellar crystals and its stress is almost equal to the necking stress. The third yielding is associated with the deformation of the glassy amorphous chains between the separated lamellae. The temperature dependence of the yield strain was in the same order as the thermal expansion coefficient of polypropylene. On the unloading curve above T_g, the plateau-like recovery region can be considered as a result of the thermal expansion stress due to the entropic behaviour of amorphous molecules between lamellae. At the end of the unloading curve above T_g, the highly strained amorphous chains between lamellae will be relaxed and subsequently crystallized to the a^*-axis oriented crystals, or the inclined a^*-axis oriented crystals will rotate perpendicular to the lamellar surface. Such a^*-axis oriented crystals can contribute to the cascade-like stress reduction at the end of the unloading curve above T_g.

REFERENCES

1 Dees, J. R. and Spruiell, J. E. *J. Appl. Polym. Sci.* 1974, **18**, 1053
2 Keller, A. and Machin, M. J. *J. Macromol. Sci. Phys.* 1967, **B1**, 41
3 Garber, C. A. and Clark, E. S. *J. Macromol. Sci. Phys.* 1970, **B4**, 499
4 Cannon, C. L., McKenna, G. B. and Statton, W. O. *J. Polym. Sci. Macromol. Rev.* 1975, **15**, 633
5 Park, I. K. and Noether, H. D. *Colloid Polym. Sci.* 1975, **253**, 824
6 Sprague, B. S. *J. Macromol. Sci. Phys.* 1973, **B8**, 157
7 Samuels, R. J. *J. Polym. Sci. Phys. Edn* 1979, **17**, 535
8 Goritz, D. and Muller, F. H. *Colloid Polym. Sci.* 1975, **253**, 844
9 Miles, M. J., Petermann, J. and Gleiter, H. *J. Macromol. Sci. Phys.* 1976, **B12**, 523
10 Noether, H. D. and Whitney, W. *Kolloid-Z.U.Z. Polym.* 1973, **251**, 991
11 Shimizu, J., Okui, N. and Imai, Y. *Sen-i Gakkaishi* 1980, **36**, T-166
12 Shimizu, J., Okui, N. and Kikutani, T. in 'High Speed Fiber Spinning' (Eds A. Ziabicki and H. Kawai), John Wiley, New York, 1985, Ch. 7, 15
13 Shimizu, J., Okui, N. and Imai, Y. *Sen-i Gakkaishi* 1979, **35**, T-405
14 Quirk, R. P. and Alsamarraie, M. A. A. in 'Polymer Handbook', 3rd Edn (Eds J. Brandrup and E. H. Immergut), John Wiley, New York, 1989
15 Wool, R. *J. Polym. Sci. Phys. Edn* 1976, **14**, 603
16 Lohse, D. J. and Gaylord, R. J. *Polym. Eng. Sci.* 1978, **18**, 512
17 Ward, I. M. 'Mechanical Properties of Solid Polymers', John Wiley, New York, 1979, Ch. 11
18 Hartmann, B., Lee, G. F. and Wong, W. *Polym. Eng. Sci.* 1987, **27**, 823
19 Brown, N., Duckett, R. A. and Ward, I. M. *Phil. Mag.* 1968, **18**, 423
20 Sakurada, I., Ito, T. and Nakamae, K. *J. Polym. Sci.* 1966, **C15**, 75
21 Tobolsky, A. V. and Takahashi, M. *J. Appl. Polym. Sci.* 1963, **7**, 1341
22 Sawatari, C. and Matuo, S. *Macromolecules* 1989, **22**, 2968
23 Miles, M. J. and Baer, E. *J. Mater. Sci.* 1979, **14**, 1254